



MR features of small hepatocellular carcinoma in normal, fibrotic, and cirrhotic livers: a comparative study

Ruo Fan Sheng,^{1,2,3} Meng Su Zeng,^{1,2,3} Yuan Ji,⁴ Li Yang,^{1,2,3} Cai Zhong Chen,^{1,2,3} Sheng Xiang Rao^{1,2,3}

¹Department of Radiology, Zhongshan Hospital, Fudan University, No. 180 Fenglin Road, Xuhui District, 200032 Shanghai, China

²Shanghai Institute of Medical Imaging, Shanghai, China

³Department of Medical Imaging, Shanghai Medical College, Fudan University, No. 180 Fenglin Road, Xuhui District, 200032 Shanghai, China

⁴Department of Pathology, Zhongshan Hospital, Fudan University, No. 180 Fenglin Road, Xuhui District, 200032 Shanghai, China

Abstract

Purpose: The objective of this study is to compare MR imaging features of small hepatocellular carcinoma (HCC) (≤ 2 cm) in normal, fibrotic, and cirrhotic liver.

Methods: A total of 215 patients with 235 pathologically proven sHCC were retrospectively analyzed. Patients were classified into three groups according to the patients' liver condition: patients with normal liver (F0, group 1), fibrosis without cirrhosis (F1–3, group 2), and cirrhosis (F4, group 3). The morphological and MR signal features on T1, T2-weighted, dynamic enhanced, and diffusion-weighted imaging were evaluated and compared.

Results: There were 10, 38, and 167 patients in group 1, 2, and 3, respectively. Patients with normal liver were older than those with fibrosis or cirrhosis ($P = 0.0086$), and tumors in the normal liver were larger than those in the fibrotic or cirrhotic liver ($P = 0.0407$). No statistical differences were found among groups in signals on T2-weighted images ($P = 0.163$), signals on each phase after contrast ($P = 0.269, 0.893, \text{ and } 0.259$, respectively), enhancement patterns ($P = 0.753$), ADC values ($P = 0.760$), as well as the presence of capsule-like enhancement ($P = 0.953$), mosaic pattern ($P = 0.572$), fat content ($P = 0.222$), iron sparing ($P = 1.000$), hemorrhage ($P = 0.181$), and venous invasion ($P = 0.175$). Both signal-to-noise ratios (SNR) ($\chi^2 = 2.045, P = 0.132$)

and lesion-to-liver contrast-to-noise ratios (CNR) ($\chi^2 = 0.438, P = 0.646$) were not different as well. But confusing features of iso/hypointensity on T2-weighted imaging ($n = 11, 6.0\%$) and progressive enhancement pattern ($n = 2, 1.1\%$) were exclusively found in the cirrhosis background, and hypovascular tumors with iso/hypointensity on arterial phase were only seen in the fibrosis ($n = 5, 11.9\%$) and cirrhosis groups ($n = 10, 5.5\%$).

Conclusion: MR features of sHCC were similar among patients with normal, fibrotic, and cirrhotic livers.

Key words: Hepatocellular carcinoma—Cirrhosis—Fibrosis—Magnetic resonance imaging

Primary liver cancer is the fifth most frequently diagnosed cancer in men (seventh in women) and the second most frequent cause of cancer death (sixth in women) worldwide, among which hepatocellular carcinoma (HCC) is the most common type and its incidence has significantly increased in recent decades [1]. Approximately 70–90% of HCCs worldwide develop within an established background of chronic liver disease and the evolving fibrosis/cirrhosis.

HCC can be diagnosed using dynamic CT or MRI based on the latest AASLD practice guidelines [2]. Classical HCC appears as a round tumor showing intense enhancement on arterial phase, and contrast washout during portal or delayed phases [3], but application to the non-cirrhotic lesions was not reported.

While at the same time, tumor characterization may be hampered by the distortion of the hepatic parenchyma and liver inhomogeneity due to the fibrotic process, and typical MRI findings of HCC are infrequently seen in lesions less than 2 cm [4–6]. Lewis et al. [7]. pointed out that HCC developed in patients with chronic HCV without advanced fibrosis or cirrhosis usually presented a typical washin-washout enhancement pattern, Lin et al. [8]. indicated that the sensitivity of HCC diagnosis by imaging was not influenced by the cirrhotic background. In addition, the presence of fibrosis/cirrhosis may be one of the most important predictor of death, and tumors arising in a non-cirrhotic, non-fibrotic liver were associated with a good prognosis [9]. Thus, accurate characterization of sHCC in patients with and without fibrosis/cirrhosis can improve diagnostic accuracy as well as provide guidance for clinical treatment and long-term prognosis.

A meta-analysis recently published pointed out that dynamic contrast-enhanced MR imaging has moderate sensitivity and excellent specificity in the detection of HCC up to 2 cm [10], but it is unclear whether imaging appearances of sHCC would be influenced by the extratumoral parenchyma; and to our knowledge, there was no published study that focused on their comparison especially based on the LI-RADS 2014 diagnostic algorithm [11]. Therefore, the purpose of our study was to compare MR imaging features of sHCC in normal, fibrotic, and cirrhotic liver.

Materials and methods

Patients

Patients were retrospectively identified by searching our institution's pathology database between January 2011 and December 2013. The pathologic diagnosis was reviewed by a pathologist with interest in liver disease and 20 years of experience. The inclusion criteria were (a) pathologically proven sHCC less than 2 cm; (b) abdominal contrast-enhanced MRI performed in our institution with satisfied image quality following standard protocol within 10 days prior to hepatectomy or biopsy; (c) no history of prior oncologic treatment or liver resection. In addition, viral hepatitis B and/or C were the only underlying liver diseases allowed in our study.

A total of 215 patients (190 men and 25 women; mean age, 54.8 year old) with sHCC were included according to the inclusion criteria. The histopathologic diagnosis of HCC was confirmed by surgical resection ($n = 206$), orthotopic liver transplantation ($n = 5$) or percutaneous biopsy ($n = 4$). The vast majority of patients were symptomless ($n = 177$) at the time of initial medical evaluation, and the most common complaint was abdominal discomfort ($n = 26$). Patient characteristics

including the age, sex, Child-Pugh grading, TNM staging (UICC/AJCC,2010), and the alpha-fetoprotein (AFP) values were assessed.

Image acquisition

MRI was performed using a 1.5-Tesla (T) scanner (Avanto; Siemens, Erlangen, Germany) with a peak gradient amplitude of 45 mT/m. An eight-channel torso phased-array coil was centered over the liver. The conventional MR protocol used in this study included transverse respiratory-navigated T2-weighted fat-suppressed turbo spin-echo sequence (TR/TE = 3500/84 ms; section thickness, 5 mm; and intersection gap, 1 mm; matrix, 168 × 320); transverse T1-weighted in-phase and opposed-phase gradient echo (TR/TE = 6.8/2.35 (in-phase), 4.75 (opposed-phase) ms; section thickness, 5 mm; intersection gap, 1 mm; matrix, 180 × 320). Diffusion-weighted imaging (DWI) was required with a transverse single-shot spin-echo echo-planar sequence (TR/TE = 2400/66 ms; section thickness, 5 mm; intersection gap, 1 mm; matrix, 168 × 320) with two b values (0 and 500 s/mm). Dynamic imaging was performed with transverse and coronal breath-hold T1-weighted 3-dimensional volumetric interpolated body examination sequence (TR/TE = 5.0/2.3 ms; section thickness, 5 mm; no intersection gap; matrix, 270 × 360) following the intravenous administration of gadopentetate dimeglumine (Magnevist; Bayer HealthCare, Berlin, Germany). Gadopentetate dimeglumine was administered at a dose of 0.1 mmol/kg at a rate of 2 mL/s, followed by a 20 mL saline flush using a power injector (Spectris; Medrad, Pittsburgh, PA). The arterial phase acquisition was triggered automatically when contrast media reached the ascending aorta. For subsequent acquisition, dynamic T1-weighted MRI at 60 s (the portal venous phase) and 90 s (the delay phase) was performed. The field of view was optimized to the patients' body habitus at 285 × 214–308 × 380 mm³.

Image analysis

All images were evaluated using a picture archiving and communication system (PACS; Pathspeed, GE Medical Systems Integrated Imaging Solutions, Prospect, IL, USA). MR findings were retrospectively and independently analyzed by two abdominal radiologists (M.S.Z. and R.F.S. with 29 and 5 years of experience in abdominal imaging, respectively) in a blinded manner. The reviewers knew that the patients had liver tumors but were unaware of all other information regarding patients' history, laboratory, and final pathological results. The MR images of sHCC were presented randomly to create the setting of clinical practice to avoid bias. As for multiple nodules, only lesions in different segments without a dominant mass were analyzed and thus were

not read as peripheral satellite nodules. The MR images were compared one by one according to the lesion size and location so as to ensure that the nodule analyzed was the same that resected or biopsied.

Qualitative analysis

For the morphological features, the observers measured the tumor size (maximal diameter), number (single/multiple), contour (round/lobulated or irregular), and location (left/right/caudal lobe).

For the signal features, Signals on T2-weighted images were defined as (a) homogeneously hyperintense; (b) heterogeneously hyperintense; (c) iso- or hypointense. Signals on each different phase after contrast administration were registered as (a) globally hyperintense; (b) partially hyperintense; (c) circularly hyperintense (d) isointense; (e) hypointense. Dynamic enhancement patterns were defined as (a) progressive: the range or intensity of enhancement progressed over time, including centripetal enhancement; (b) persistent: the enhancement remained invariable through all three phases; (c) degressive (wash-in without wash-out): decreasing hyperintensity over time without hypointense appearance on portal or delayed phases; (d) wash-in with wash-out: contrast uptake during arterial phase followed by contrast washout which showed relative hypointensity on portal or delayed phases.

According to the LI-RADS 2014 diagnostic algorithm [11], accompanying imaging findings including the presence of capsule-like enhancement, corona enhancement, mosaic pattern, fat content, iron sparing, hemorrhage and venous invasion were also measured. Capsule-like enhancement was defined as a thin rim-like enhancement along the periphery of the tumor during the portal or delayed phases. Corona enhancement was considered if the rim enhancement occurred on the arterial phase and then faded. Mosaic pattern was presented as heterogeneity within lesions. Fat content was diagnosed if in-phase and opposed-phase signal dropout. Iron deposition appeared as decreased signal intensity scattered diffusely within the lesion on T2WI. Intratumoral hemorrhage was defined as linear, dot-like or patchy hypointensity on T2WI [12].

Quantitative analysis

As the qualitative analyses of the signal features reflected the enhancement modes of lesions; while the quantitative analyses of signal-to-noise ratio (SNR) and lesion-to-liver contrast-to-noise ratio (CNR) reflected the enhancement degree of lesions. We calculated both the qualitative and quantitative enhanced signal features. Signal intensity (SI) of the tumor, liver parenchyma, and standard deviation (SD) of the background noise during dynamic enhanced imaging were recorded using a region

of interest (ROI). In ROI placement of the lesion, the enhanced portion within the tumor as large as possible was chosen, and the ROI of the liver parenchyma was set in the same slice where the ROI of the lesion was set, great care was taken to avoid large vessels, necrosis, hemorrhage, and artifacts. ROIs were placed in identical locations and in similar size for each sequence. SNR was defined as $SI_{\text{lesion}}/SD_{\text{noise}}$. CNR was defined as $(SI_{\text{lesion}} - SI_{\text{liver}})/SD_{\text{noise}}$. Regarding the measurement of the apparent diffusion coefficient (ADC) values, ROI was manually drawn on the diffusion-weighted images, these ROIs were then copied onto the ADC maps, and the ADC values were assessed. Two measurements were taken for each ROI by one radiologist (R.F.S), and the average was used for analysis.

Pathological analysis

All pathologic specimens were reviewed by a pathologist (Y.J., with 20 years of experience in liver pathology). Liver fibrosis was staged according to a METAVIR-equivalent score from F0 to F4: F0, no fibrosis; F1, portal fibrosis without septa; F2, portal fibrosis and few septa; F3, numerous septa without cirrhosis; and F4, cirrhosis [13]. Liver fibrosis grading was done at the same time and using the same needle biopsy or surgical specimen used to diagnose the liver mass as HCC. The patients were further classified into three groups: patients with neither liver fibrosis nor cirrhosis (F0, group 1), patients with fibrosis without cirrhosis (F1-3, group 2), and patients with cirrhosis (F4, group 3). Histological grading (Edmondson-Steiner grade) [14] of the tumors was also analyzed.

Statistical analysis

All statistical analyses were performed using SPSS 20.0 (Chicago, IL, USA). Continuous variables were compared with the Kruskal–Wallis test. Categorical variables were compared using Fisher's exact test. The mean ADC values of the lesion and liver parenchyma was compared using a paired *t* test. The repeated-measures analysis of variance model was used to compare the SNR and CNR during dynamic enhanced scanning. The pairwise comparison of individual mean differences was evaluated by using the least significant difference (LSD) post hoc test or Dunn's multiple comparison test. Interobserver agreements regarding the categorical variables were evaluated by using κ statistics. The agreement was rated on the following scale: $\kappa = 0-0.20$, slight agreement; $0.21-0.40$, fair agreement; $0.41-0.60$, moderate agreement; $0.61-0.80$, substantial agreement; and 0.81 or greater, excellent agreement [15]. In cases of disagreement, a third observer (L.Y.) was asked for an opinion, and a majority decision was reached and used for data

Table 1. Main patient characteristics

Characteristic	Group 1	Group 2	Group 3	<i>P</i>
Age (years) ^a	65.0 (48.0, 70.5)	52.5 (42.8, 58.3)	56.0 (49.0, 61.0)	0.0086
Sex male/female	9/1	35/3	146/21	0.836
Child-pugh A/B	10/0	38/0	164/3	1.000
AFP > 20 ng/mL Yes/No	5/5	19/19	89/78	0.931
TNM staging (UICC/AJCC,2010) I/II/III	6/4/0	25/7/6	112/43/12	0.302
Lesion histological grading I/II/III	0/9/1	3/32/7	3/134/46	0.193

Unless otherwise specified, data are numbers of patients/lesions

AFP alpha-fetoprotein

^a Data are median, with interquartile range in parentheses

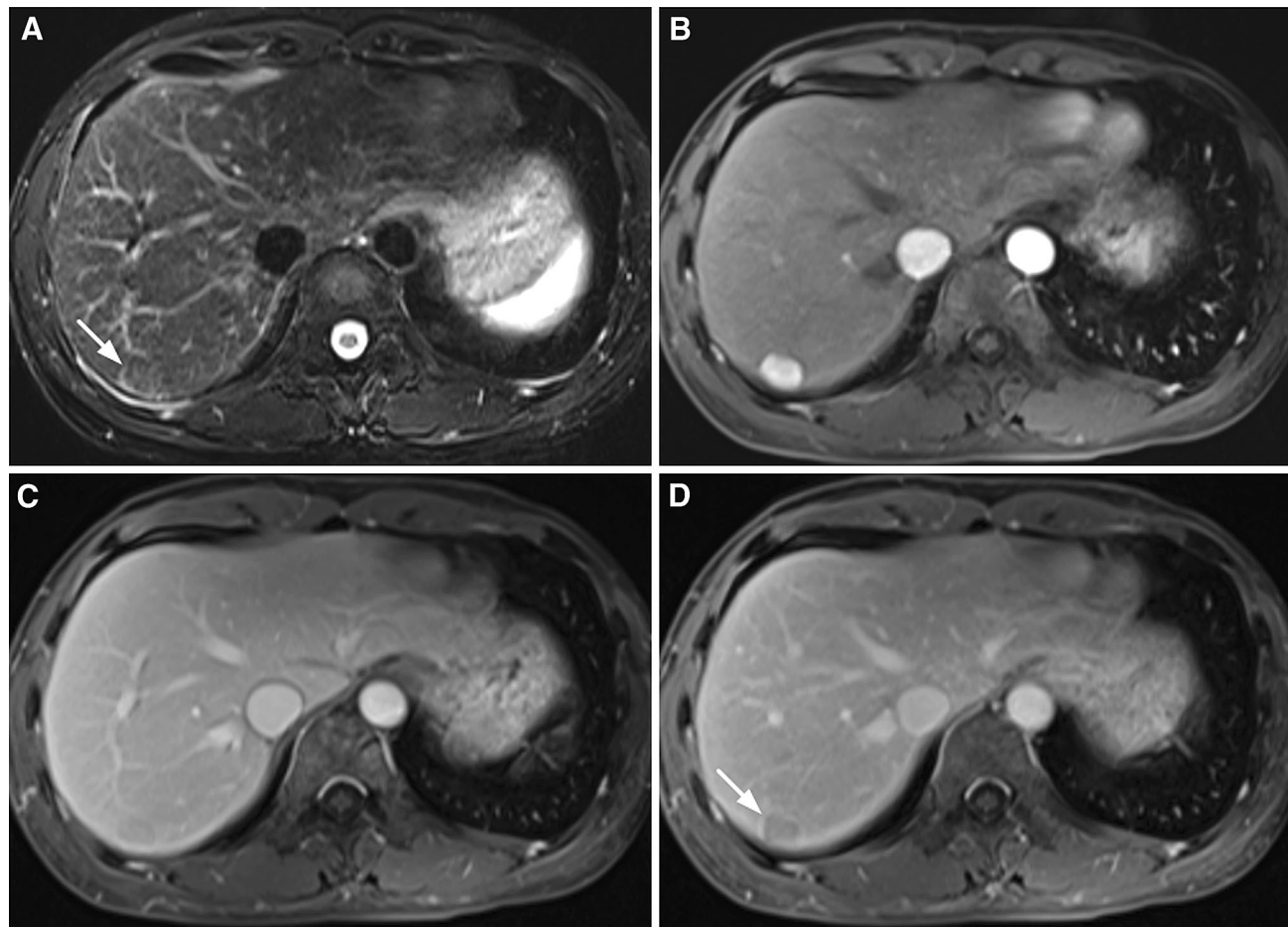


Fig. 1. Small hepatocellular carcinoma in a 40-year-old man with cirrhosis. **A** Transverse T2-weighted image showed a round tumor with isointensity (*arrow*). Transverse T1-weighted VIBE images showed **(B)** global hyperintensity on arterial

phase and **(C, D)** a wash-out enhancement pattern with hypointensity on portal and delayed phases. Note the accompanying capsule-like enhancement on delayed phase (*arrow*).

analysis. All tests were two-sided and $P < 0.05$ was considered statistically significant.

Results

Patient characteristics

The final study group comprised 215 patients with 235 SHCC. There were 10, 38, and 167 patients in group 1, 2,

and 3, respectively. Patients were predominantly male, and patients with normal liver were older than those with fibrosis or cirrhosis ($P = 0.0086$). Evidence of hepatic B and C viral infection was identified in 206 and 3 patients, respectively, the other 6 patients had no underlying liver disease. Among all patients, only half had an elevated AFP with no differences among the three groups ($P = 0.931$). 6/175/54 lesions were diagnosed as E–S

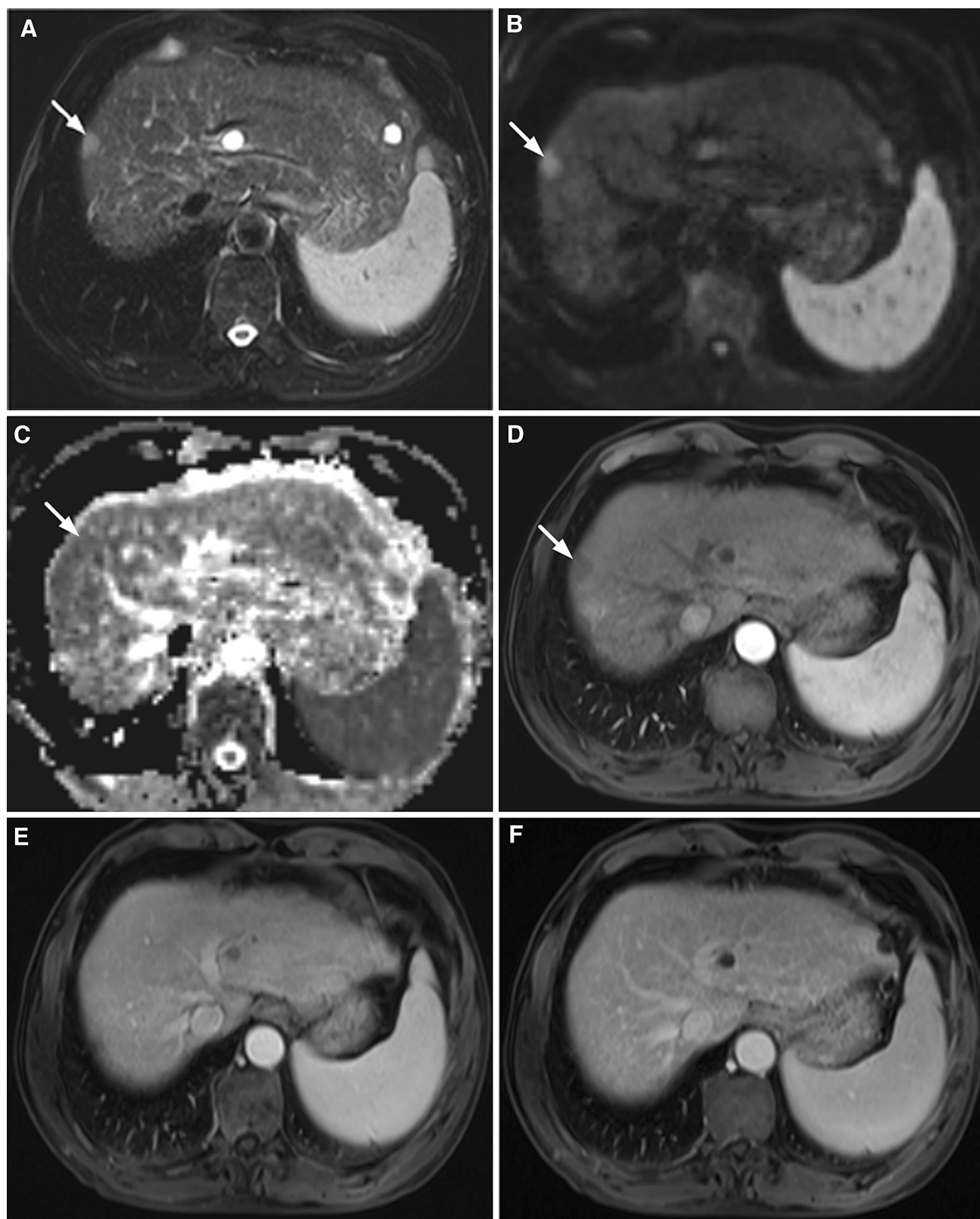


Fig. 2. Small hepatocellular carcinoma in a 64-year-old man with cirrhosis. **A** Transverse T2-weighted image showed a round tumor with homogenous hyperintensity (*arrow*). **B** Diffusion-weighted image showed hyperintensity and **C** ADC map

showed mild hypointensity of the lesion (*arrow*). Transverse T1-weighted VIBE images showed **D** relative hypointensity on arterial phase (*arrow*) and **E**, **F** a progressive enhancement pattern with global isointensity on portal and delayed phases.

Table 2. Main tumor MR characteristics

Variable	Group 1	Group 2	Group 3	<i>P</i>
Signal on T2-weighted images				0.163
Homogenous hyperintense	2	21	88	
Heterogeneous hyperintense	8	21	84	
Iso- or hypointense	0	0	11	
Signal on arterial phase				0.269
Globally hyperintense	7	29	128	
Partially hyperintense	3	8	29	
Circularly hyperintense	0	0	16	
Isointense	0	4	7	
Hypointense	0	1	3	
Dynamic enhancement pattern				0.753
Progressive	0	0	2	
Persistent	2	10	31	
Degressive	4	11	47	
Wash-in with wash-out	4	21	103	
Capsule-like enhancement Y/N	8/2	33/9	138/45	0.953
Corona enhancement Y/N	3/7	12/30	37/146	0.381
Mosaic pattern Y/N	4/6	10/32	50/133	0.572
Fat content Y/N	3/7	4/38	26/157	0.222
Iron sparing Y/N	10/0	42/0	182/1	1.000
Hemorrhage Y/N	2/8	3/39	32/151	0.181
Venous invasion Y/N	3/7	4/38	34/149	0.175

Data are numbers of lesions

grading I/II/III, respectively, and no differences were found ($P = 0.193$) (Table 1).

MRI findings

Morphological characteristics

Tumors in the normal liver were larger than those in the fibrotic or cirrhotic liver ($P = 0.0407$), but the result may be artificially constrained due to the inclusion criteria in this study. Other morphological features including the nodule number ($P = 0.798$), contour ($P = 0.835$), and location ($P = 0.397$) were not different among groups.

MR signal characteristics

No statistical difference was found when comparing the signal intensity on T2-weighted imaging ($P = 0.163$), but iso- or hypointense lesions were all in the cirrhosis group ($n = 11$, 6.0%; Fig. 1A).

The majority of tumors were hypervascular, while iso- or hypointense tumors on arterial phase can also be found in the fibrosis ($n = 5$, 11.9%) and cirrhosis groups ($n = 10$, 5.5%; Fig. 2D). There were no statistical differences in term of enhancement patterns ($P = 0.753$) and signals on each phase ($P = 0.269$, 0.893, 0.259), although the progressive pattern only existed in the cirrhotic liver ($n = 2$, 1.1%; Fig. 2D–F); and both SNR ($\chi^2 = 2.045$, $P = 0.132$) and CNR ($\chi^2 = 0.438$, $P = 0.646$) were not different among groups as a whole (Table 2).

There were no differences with regard to the accompanying imaging findings including the presence of capsule-like enhancement ($P = 0.953$; Fig. 1D), mosaic pattern

($P = 0.572$; Fig. 3C–E), fat content ($P = 0.222$), iron sparing ($P = 1.000$), hemorrhage ($P = 0.181$; Fig. 3A, B), and venous invasion ($P = 0.175$) (Table 2).

On DWI, all lesions were hyperintense in varying degrees (Fig. 2B), the mean ADC value of the lesions was lower than that of surrounding liver (Fig. 2C; $t = 12.02$, $P < 0.001$); but the absolute ADC values of the lesions were not different among the three groups ($P = 0.760$).

Excellent agreement between the two observers was obtained for all measured categorical parameters ($\kappa = 0.803$ –0.989).

Discussion

In our study, sHCC was male predominance and patients with normal liver background had older ages, these were consistent with the study of Lewis et al. [7]. But some researches reported that HCC in the non-cirrhotic liver occurred in younger patients [8, 16], these discrepancies may be caused by the different disease cause and ethnic constitution. In addition, our results showed that tumors in the fibrotic and cirrhotic liver were smaller than those in the normal liver, which may be related to a more frequent follow-up in these patients, but this result may be largely influenced by the artificial constraint of the inclusion criteria, as only lesions less than 2 cm were included.

MRI provides satisfied soft-tissue contrast and plays a crucial role in the detection and diagnosis of sHCC [10]. The current 2011 AASLD recommendations propose that HCC with typical contrast enhancement pattern can be diagnosed by MRI [2]. However, these diagnostic criteria were not approved for patients with non-cirrhotic livers. Therefore, there are difficulties in diagnosing HCC and differentiating them from other entities such as adenoma, hemangioma, hypervascular metastases which can represent a source of false positive findings in clinical practice for these patients. Meanwhile, Liver inhomogeneity due to fibrosis and the change in distribution of blood flow in the cirrhotic liver may lead to heterogeneous MR signal intensity, which may significantly impair lesional visibility and alter lesion manifestation.

In our study, we found that most sHCC presented typical MR features of T2-hyperintensity, contrast uptake on arterial phase and contrast washout with the capsule-like enhancement during portal or delayed phases; other accompanying findings including the corona enhancement, mosaic pattern, fat content, iron sparing, and intralesional hemorrhage were not rarely seen, regardless of the hepatic parenchyma background. Our findings are similar to prior studies of HCC with a variety of underlying risk factors [7, 8, 17].

Confusing features in sHCC as iso/hypointensity on T2WI and progressive enhancement pattern were exclusively found in the cirrhosis background, and hypovascular tumors with iso/hypointensity on arterial phase were only seen in the fibrosis and cirrhosis group. These

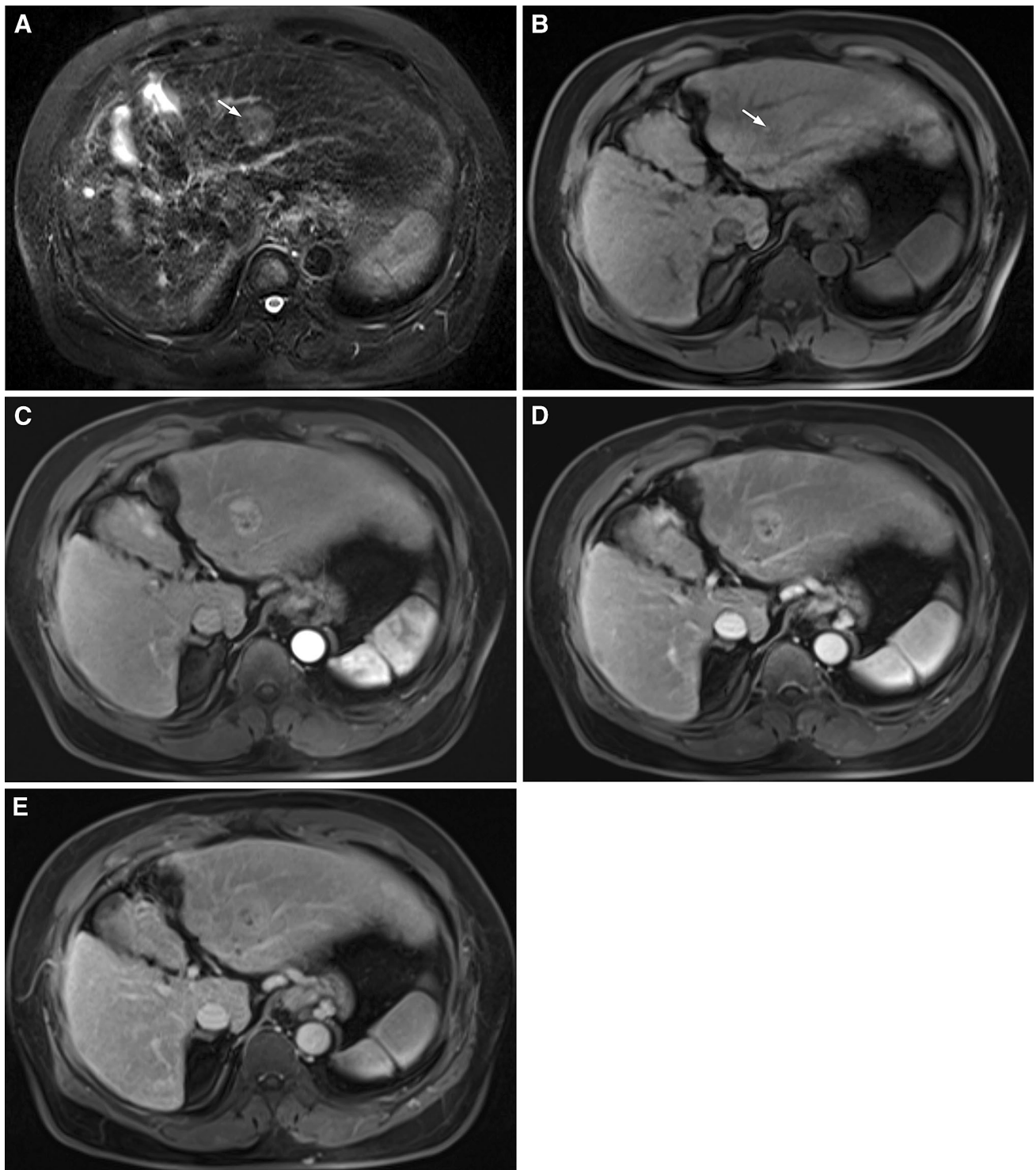


Fig. 3. Small hepatocellular carcinoma in a 55-year-old man with cirrhosis. **A** Transverse T2-weighted image showed a hyperintense tumor with few hypointensity indicating intratumoral hemorrhage (*arrow*). **B** Transverse T1-weighted VIBE image showed a mild hypointense tumor with few hyperin-

tensity (*arrow*). Transverse T1-weighted VIBE images showed **C**, **D** heterogeneous hyperintensity with a mosaic pattern on arterial and portal phases and **E** a degressive enhancement pattern with heterogeneous isointensity on delayed phase.

may be related to the distortion of the hepatic parenchyma due to the fibrotic process and the particular profile caused by portal hypertension and associated

circulatory disturbances [18]. Decreased blood supply or reduced sinusoidal space was thought to be responsible for hypo/isointensity on T2-weighted images [19]. In

addition, the relative small lesion size may partially explain the atypical manifestations above, due to the residual portal venous supply or incomplete neovascularization [5, 6, 20]. But we should recognize that despite all these differences between lesions in normal and fibrosis/cirrhosis background, none of them were statistically significant. Thus, a combination of the clinical features and other MR sequences would be of great value, and further researches are needed to achieve more convincing conclusions.

DWI provides insights into the molecular water composition and may provide information regarding the cellular density and properties of the extracellular matrix [21]. All lesions were hyperintense in varying degrees, the restricted diffusion favors the diagnosis of HCC. However, DWI is hampered by the low specificity, and there are substantial overlaps in the range of ADCs among sHCC in normal, fibrotic, and cirrhotic liver. Thus, its use in differentiation may be limited, and they should be interpreted concurrently with other MR sequences to make an exact radiologic diagnosis.

This study had several limitations. First, our study was a retrospective research, thus selection bias may exist. Second, the study population of the normal group and fibrosis group was relatively small, thus thorough analysis between different stages of liver fibrosis was not achieved, further prospective study with larger sample size would be necessary. Third, a precise correlation between the imaging findings and the overall histopathological composition was not made, further point-to-point radiologic-pathologic correlation studies are needed. Fourth, our study mainly discussed the key points of differentiating the MR features of sHCC with varying degrees of fibrosis, the differentiation of sHCC from other benign and malignant entities such as adenoma, hemangioma, and hypervascular metastases was not analyzed in detail and needs further researches. Finally, we used traditional extracellular contrast agent (Gadopentetate dimeglumine). Nowadays, liver-specific contrast agents (e.g., Gadoxetic acid) are increasingly used for detection and characterization of focal liver lesions, and hypointensity on hepatobiliary phase favor HCC [11], further studies are needed to confirm their potential advantages in the differentiation of sHCC with varying degrees of fibrosis.

In conclusion, MR features of sHCC were similar among patients with normal, fibrotic, and cirrhotic livers, although atypical features of iso/hypointensity on T2WI, iso/hypointensity on arterial phase, and progressive enhancement pattern were exclusively found in the fibrosis and cirrhosis groups.

References

1. Jemal A, Bray F, Center MM, et al. (2011) Global cancer statistics. *Cancer J Clin* 61:69–90
2. Bruix J, Sherman M (2011) Management of hepatocellular carcinoma: an update. *Hepatology* 53:1020–1022
3. Forner A, Vilana R, Ayuso C, et al. (2008) Diagnosis of hepatic nodules 20 mm or smaller in cirrhosis: prospective validation of the noninvasive diagnostic criteria for hepatocellular carcinoma. *Hepatology* 47:97–104
4. Hanna RF, Aguirre DA, Kased N, et al. (2008) Cirrhosis-associated hepatocellular nodules: correlation of histopathologic and MR imaging features. *Radiographics* 28:747–769
5. Willatt JM, Hussain HK, Adusumilli S, Marrero JA (2008) MR Imaging of hepatocellular carcinoma in the cirrhotic liver: challenges and controversies. *Radiology* 247:311–330
6. Kim I, Kim MJ (2012) Histologic characteristics of hepatocellular carcinomas showing atypical enhancement patterns on 4-phase MDCT examination. *Korean J Radiol* 13:586–593
7. Lewis S, Roayaie S, Ward SC, et al. (2013) Hepatocellular carcinoma in chronic hepatitis C in the absence of advanced fibrosis or cirrhosis. *Am J Roentgenol* 200:W610–W616
8. Lin M-T, Chen C-L, Wang C-C, et al. (2011) Diagnostic sensitivity of hepatocellular carcinoma imaging and its application to non-cirrhotic patients. *J Gastroenterol Hepatol* 26:745–750
9. Truant S, Boleslawski E, Duhamel A, et al. (2012) Tumor size of hepatocellular carcinoma in noncirrhotic liver: a controversial predictive factor for outcome after resection. *Eur J Surg Oncol* 38:1189–1196
10. Kierans AS, Kang SK, Rosenkrantz AB (2015) The diagnostic performance of dynamic contrast-enhanced MR imaging for detection of small hepatocellular carcinoma measuring up to 2 cm: a meta-analysis. *Radiology*. doi:10.1148/radiol.2015150177
11. Mitchell DG, Bruix J, Sherman M, Sirlin CB (2015) LI-RADS (Liver Imaging Reporting and Data System): summary, discussion, and consensus of the LI-RADS Management Working Group and future directions. *Hepatology* 61:1056–1065
12. Anis M (2015) Imaging of hepatocellular carcinoma: new approaches to diagnosis. *Clin Liver Dis* 19:325–340
13. Bedossa P, Poynard T (1996) An algorithm for the grading of activity in chronic hepatitis C. *Hepatology* 24:289–293
14. Edmondson HA, Steiner PE (1954) Primary carcinoma of the liver: a study of 100 cases among 48,900 necropsies. *Cancer* 7:462–503
15. Landis JR, Koch GG (1977) Measurement of observer agreement for categorical data. *Biometrics* 33:159–174
16. Alkofer B, Lepennec V, Chiche L (2011) Hepatocellular cancer in the non-cirrhotic liver. *J Visc Surg* 148:3–10
17. Rimola J, Forner A, Tremosini S, et al. (2012) Non-invasive diagnosis of hepatocellular carcinoma \leq 2 cm in cirrhosis. Diagnostic accuracy assessing fat, capsule and signal intensity at dynamic MRI. *J Hepatol* 56:1317–1323
18. Rimola J, Forner A, Reig M, et al. (2009) Cholangiocarcinoma in cirrhosis: absence of contrast washout in delayed phases by magnetic resonance imaging avoids misdiagnosis of hepatocellular carcinoma. *Hepatology* 50:791–798
19. Matsui O, Kadoya M, Kameyama T, et al. (1989) Adenomatous hyperplastic nodules in the cirrhotic liver: differentiation from hepatocellular carcinoma with MR imaging. *Radiology* 173:123–126
20. Willatt JM, Hussain HK, Adusumilli S, Marrero JA (2008) MR Imaging of hepatocellular carcinoma in the cirrhotic liver: challenges and controversies. *Radiology* 247:311–330
21. Vossen JA, Buijs M, Liapi E, et al. (2008) Receiver operating characteristic analysis of diffusion-weighted magnetic resonance imaging in differentiating hepatic hemangioma from other hypervascular liver lesions. *J Comput Assist Tomogr* 32:750–756